

Magnetic Solitons in a Binary Bose-Einstein Condensate

Chunlei Qu¹, Lev P. Pitaevskii^{1,2}, and Sandro Stringari¹

¹*INO-CNR BEC Center and Dipartimento di Fisica, Università di Trento, 38123 Povo, Italy*

²*Kapitza Institute for Physical Problems RAS, Kosygina 2, 119334 Moscow, Russia*

(Dated: September 25, 2018)

We study solitary waves of polarization (magnetic solitons) in a two-component Bose gas with slightly unequal repulsive intra- and interspin interactions. In experimentally relevant conditions we obtain an analytical solution which reveals that the width and the velocity of magnetic solitons are explicitly related to the spin healing length and the spin sound velocity of the Bose mixture, respectively. We calculate the profiles, the energy and the effective mass of the solitons in the absence of external fields and investigate their oscillation in a harmonic trap where the oscillation period is calculated as a function of the oscillation amplitude. The stability of magnetic solitons in two dimensions and the conditions for their experimental observation are also briefly discussed.

PACS numbers: 03.75.Lm, 03.75.Mn, 67.85.Fg

Introduction.—Solitons, the fascinating topological excitations of nonlinear systems, have drawn a considerable research interest in many physical branches ranging from classical fluids, fibre optics [1], polyacetylene [2], magnets [3] and so on. Because of the interplay of nonlinearity and dispersion, solitons can move in their medium without losing their shape and thus have important application in information processing. Among various physical systems, ultracold atomic gases provide a prominent platform for the investigation of solitons which can be engineered by phase imprinting, density imprinting, quantum quenches, etc. Soon after the realization of Bose-Einstein condensation, dark and bright solitons characterized by density notches and density bumps have been actually observed in repulsive [4, 5] and attractive [6] interacting Bose gases, respectively.

Recently, vector solitons such as dark-dark and dark-bright soliton complexes have been explored in spinor Bose gases where the underlying physics is even richer (see, for example, reference [7]). Different techniques have been utilized to generate vector solitons in experiments with quantum mixtures. For instance, by filling the dark soliton of one species with atoms of another species [8] or by the counterflow of two superfluids [9], the dark-bright solitons are engineered and observed. Despite this experimental progress, our theoretical understanding of vector solitons mainly relies on numerical calculations and some analytical results were only obtained under stringent conditions. For example, Busch and Anglin [7] studied the dark-bright soliton under the assumption of equal spin interactions, $g_{11} = g_{22} = g_{12}$, where a dark soliton is developed in one component and filled by the atoms of another component, the density background being fully polarized (see also [10] and references therein.)

In this Letter, we investigate another type of soliton, a *magnetic soliton*, in a two-component Bose gas which exists only when the repulsive intra- and interspin interactions of the two species are unequal. Different from

dark-bright solitons, the magnetic soliton manifests itself as a localized spin polarization $n_1 - n_2$, where $n_{1,2}$ are the densities of the two components, and resides in a spin-balanced density background. To construct an explicit analytic solution, we take advantage of the fact that typical experimental mixtures of hyperfine states of bosonic alkali atoms are near the boundary of phase separation instability, that is the coupling constants satisfy the inequality:

$$\delta g \equiv g - g_{12} \ll g, \quad (1)$$

where $g = \sqrt{g_{11}g_{22}}$ and $\delta g > 0$ in order to avoid phase separation. For instance, considering the two hyperfine states $|F = 1; m_F = \pm 1\rangle$ of ^{23}Na , one has $g_{11} = g_{22}$ and $\delta g/g \approx 0.07$ [11, 12]. The inequality (1) is crucial in order to ensure the decoupling between density and spin dynamics. In particular it ensures that the total density $n = n_1 + n_2$ is practically unperturbed in the region of the magnetic soliton and one can safely assume $n = \text{const}$ (see discussion below). A theory of weakly-nonlinear polarization waves in two-component Bose gases was developed in [13] beyond the condition of Eq. (1).

Similarly to a regular dark soliton, the magnetic soliton is expected to show snake instability when the transverse size becomes larger than the width of the soliton, due to its negative effective mass. However, since the spin healing length is large in spinor Bose gases under the condition (1), the magnetic solitons are more resilient against instability than dark solitons whose width is fixed by the smaller density healing length. For the same reason they can be wide enough to be observed directly in *in situ* measurements. Finally, we calculate the oscillation frequency of the magnetic solitons with arbitrary oscillation amplitudes in a harmonic trap which may be a useful benchmark for the observation in real experiments.

Densities and phases.—We consider a two-component Bose-Einstein condensate at $T = 0$. The system is governed by two coupled Gross-Pitaevskii equations (GPE) which can be obtained from the Lagrangian density $\mathcal{L} =$

$\sum_{j=1,2} \frac{i\hbar}{2} (\psi_j^* \partial_t \psi_j - \psi_j \partial_t \psi_j^*) - \mathcal{E}$, where ψ_j is the condensate wave function for the j th component and the energy density is given by

$$\mathcal{E} = \sum_j \left[\frac{\hbar^2}{2m} |\nabla \psi_j|^2 + V_{ext} |\psi_j|^2 + \sum_l \frac{g_{jl}}{2} |\psi_j|^2 |\psi_l|^2 \right], \quad (2)$$

with V_{ext} the external trapping potential. For simplicity, we will assume $g_{11} = g_{22} = g$ in the following.

We will first study magnetic solitons in the absence of the external potential ($V_{ext} = 0$). For a 1D two-component Bose gas the wave function can be parametrized as

$$\begin{pmatrix} \psi_1 \\ \psi_2 \end{pmatrix} = \sqrt{n} \begin{pmatrix} \cos(\theta/2) e^{i\varphi_1} \\ \sin(\theta/2) e^{i\varphi_2} \end{pmatrix}, \quad (3)$$

where $\varphi_{1,2}$ are the phases of the two components, n is the 1D constant total density and the spin polarization is given by $\cos \theta = (n_1 - n_2)/n$. It is also convenient to introduce the relative phase $\varphi_A = \varphi_1 - \varphi_2$ and the total phase $\varphi_B = \varphi_1 + \varphi_2$ of the two order parameters. Without any loss of generality we can assume $\varphi_{1,2} = 0$ at $z = -\infty$. In terms of these new variables, the Lagrangian can be rewritten as

$$\mathcal{L} = -\frac{n\hbar}{2} (\cos \theta \partial_t \varphi_A + \partial_t \varphi_B) - \frac{n\hbar^2}{8m} \left[2 \cos \theta \partial_z \varphi_A \partial_z \varphi_B + (\partial_z \varphi_A)^2 + (\partial_z \varphi_B)^2 + (\partial_z \theta)^2 \right] + \frac{n^2 \delta g}{4} \sin^2 \theta, \quad (4)$$

which represents a special case of the Lagrangian derived by Son and Stephanov in Ref. [14] where an additional coherent Rabi coupling was considered [15]. It is important to note that the term $\partial_t \varphi_B$, as a derivative, does not contribute to equations of motion and will be omitted.

To look for traveling soliton solutions, we substitute $\theta = \theta(z - Vt)$ and $\varphi_{A,B} = \varphi_{A,B}(z - Vt)$ in the Lagrangian which is simplified to the following form

$$\frac{\mathcal{L}}{nmc_s^2} = U (\cos \theta \partial_\zeta \varphi_A) - \frac{1}{2} [2 \cos \theta \partial_\zeta \varphi_A \partial_\zeta \varphi_B + (\partial_\zeta \varphi_A)^2 + (\partial_\zeta \varphi_B)^2 + (\partial_\zeta \theta)^2] + \frac{1}{2} \sin^2 \theta, \quad (5)$$

with $\zeta = (z - Vt)/\xi_s$, $U = V/c_s$ as the coordinate and velocity in unit of the spin healing length $\xi_s = \hbar/\sqrt{2mn\delta g}$ and spin sound velocity $c_s = \sqrt{n\delta g/2m}$, respectively.

The variation of the Lagrangian with respect to the total phase φ_B gives $\partial_\zeta (\partial_\zeta \varphi_B + \cos \theta \partial_\zeta \varphi_A) = 0$. Imposing the boundary condition $\partial_\zeta \varphi_{A,B} = 0$ at $\zeta = \pm\infty$, we can write

$$\partial_\zeta \varphi_B + \cos \theta \partial_\zeta \varphi_A = 0. \quad (6)$$

Therefore the total phase φ_B can be calculated by a simple integration once the other variables θ and φ_A are determined. With the help of Eq. (6), the Lagrangian

can be further simplified and the variation with respect to φ_A and θ gives the following two differential equations

$$\partial_\zeta \varphi_A = U \frac{\cos \theta}{\sin^2 \theta}, \quad \partial_\zeta^2 \theta = U^2 \frac{\cos \theta}{\sin^3 \theta} - \sin \theta \cos \theta, \quad (7)$$

where we have used the additional boundary condition $n_{1,2} = n/2$, i.e., $\theta = \pi/2$, at $\zeta = \pm\infty$. The density distributions of the two components can be obtained after a simple integration of the second Eq. (7) and take the form

$$n_{1,2} = \frac{n}{2} (1 \pm \cos \theta) = \frac{n}{2} \left[1 \pm \frac{\sqrt{1 - U^2}}{\cosh(\zeta \sqrt{1 - U^2})} \right]. \quad (8)$$

Without loss of generality, we will assume $n_1 \geq n_2$ in the following discussions and take + sign in Eq. (8). Substituting result (8) for θ into the first Eq. (7) and Eq. (6), the relative phase φ_A and the total phase φ_B can be readily solved:

$$\cot \varphi_A = -\sinh(\zeta \sqrt{1 - U^2})/U, \quad (9)$$

$$\tan(\varphi_B + C) = -\sqrt{1 - U^2} \tanh(\zeta \sqrt{1 - U^2})/U, \quad (10)$$

where the constant C can be chosen to ensure $\varphi_B(\zeta = -\infty) = 0$.

A typical example of the soliton density distribution is shown in Fig. 1(a) for the positive value $U = V/c_s = 0.6$ of the velocity. The figure shows that the spin polarization vanishes at large distance from the soliton. Since $0 \leq |U| \leq 1$, the velocity of the magnetic soliton cannot exceed the spin sound velocity c_s . The magnetization $(n_1 - n_2)/n$ in the center of the soliton is given by $m_0 = \sqrt{1 - U^2}$. It reaches its maximal value one for the static solution ($U = 0$), while vanishes as V approaches the spin sound velocity. In this latter limit the magnetic soliton behaves like a spin wave packet. The width of the magnetic soliton, fixed by the spin healing length ξ_s , is amplified by the factor $1/\sqrt{1 - U^2}$. Despite the fact that the central magnetization and the width of the soliton depend on its velocity, the total magnetization, defined by $\int_{-\infty}^{+\infty} dz (n_1 - n_2)/n$ is velocity independent and given by

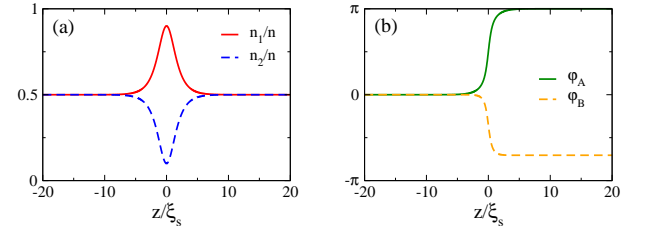


FIG. 1: Profiles of a magnetic soliton with velocity $V/c_s = 0.6$. (a) The red solid and blue dashed lines are the density distributions of the two components, satisfying $(n_1 + n_2)/n = 1$. (b) The green solid and yellow dashed lines are the relative and total phases as a function of the coordinate.

the analytic result $\pi\xi_s$. Figure 1(b) illustrates the phases of the magnetic soliton for $U = 0.6$, showing that φ_A exhibits an exact π phase jump. For negative velocities, the phase jumps of φ_A and φ_B will change sign accordingly. Figure 2(a) characterizes the relative and total phases of the magnetic solitons. Although the relative phase φ_A always has a π phase jump according to Eq. (9), its slope at the soliton center ($\partial_\zeta\varphi_A|_{\zeta=0}$) is steeper for solitons with a slower velocity and becomes a step function for the static magnetic soliton. Differently from φ_A , the asymptotic phase jump of φ_B instead varies as a function of the velocity and φ_B becomes zero for $U \rightarrow 1$.

Energy and effective mass.—Solitons can usually be described as quasiparticles where the energy plays the role of the Hamiltonian. The importance of the energy also relies on the fact that it is a useful quantity to study the dynamics of solitons in harmonic traps [17, 18]. In the case of uniform systems (no external trapping potential) the energy of the soliton can be evaluated straightforwardly as the difference between the grand canonical energies in the presence and in the absence of the soliton (see [16], Chap.5). We find $\epsilon = n\hbar c_s \sqrt{1 - V^2/c_s^2}$, which is maximal for the static soliton and vanishes when $V = c_s$. For small values of velocities, the soliton behaves like a quasi-particle with a negative effective mass $m_{eff} = -n\hbar/c_s$. Solitons with negative effective mass are not stable against nonuniform transverse snake fluctuations. When the transverse size is larger than the width of the soliton, the soliton decays into vortices as we will discuss in the following.

Using the energy ϵ , one can justify our main assumption that the total density is unaffected by the presence of a magnetic soliton. Let us consider a static soliton. Then $\epsilon = \hbar n^{3/2} \sqrt{\delta g/2m}$ and one can calculate the depletion of number of atoms in the soliton using the thermodynamic relation $N_D \equiv \int_{-\infty}^{\infty} [n(z) - n] dz = -\partial\epsilon/\partial\mu$, where $\mu = ng$ is the chemical potential. A simple calculation gives $N_D = -3n\xi_s(\delta g/2g)$. One can esti-

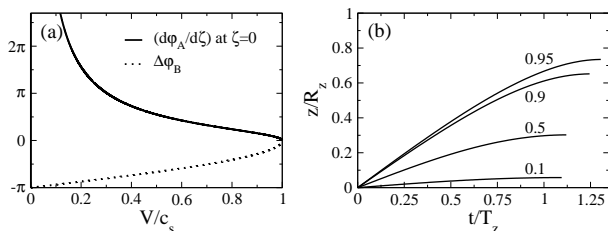


FIG. 2: (a) Velocity dependence of the soliton phases in a uniform system. The solid and dotted lines are the slope of the relative phase $d\varphi_A/d\zeta$ at $\zeta = 0$ and the increment of the total phase $\Delta\varphi_B = \varphi_B(\zeta = +\infty) - \varphi_B(\zeta = -\infty) = -2 \arccos U$. (b) Time dependence of the magnetic soliton position in a harmonic trapping potential. The four lines represent the motion of the soliton from the trap center $z = 0$ to the turning position for different initial velocities ($U_0 = 0.1, 0.5, 0.9, 0.95$).

mate the density perturbation near the soliton center as $|n(z) - n| \sim |N_D|/\xi_s \sim n\delta g/g \ll n$.

In-trap oscillations.—The particle-like nature of solitons is revealed by its long time stable oscillations in a 1D or elongated 2D harmonic traps with axial trapping frequency equal to ω_z . The oscillation period of dark solitons of a single component Bose gas in a harmonic trap is $\sqrt{2}T_z$, where $T_z = 2\pi/\omega_z$ is the oscillator period [17, 18]. For the dark-bright solitons studied in Ref. [7], the oscillation is much slower and depends on the population of the bright-soliton component.

To describe the oscillation of magnetic solitons in a harmonic trap, we consider the energy of the soliton in the local density approximation $\epsilon(z) = n(z)\hbar\sqrt{c_s^2(z) - V^2(z)}$, where $n(z)$, $c_s(z)$ and $V(z)$ are the total density, the spin sound velocity and the velocity of the magnetic soliton at position z . Let us assume that a magnetic soliton is initially engineered at $z = 0$ with energy $\epsilon_0 = n_0\hbar\sqrt{c_{s0}^2 - V_0^2}$ where n_0 , c_{s0} and $V_0 = U_0c_{s0}$ are the density, spin sound velocity and the soliton velocity at the trap center. Since the energy of the soliton remains ϵ_0 in the following evolution, the velocity is therefore evaluated as

$$V(z) = \frac{dz}{dt} = \sqrt{\frac{n(z)\delta g}{2m} - \frac{\epsilon_0^2}{n^2(z)\hbar^2}}, \quad (11)$$

where the total density at the position of the soliton can be approximated by $n(z) = n_0(1 - z^2/R_z^2)$, the Thomas-Fermi radius R_z of the condensate being given by $m\omega_z^2 R_z^2/2 = n_0g$.

The oscillation of the magnetic soliton can be explored by solving Eq. (11) with the initial condition $z(t = 0) = 0$. Figure 2(b) shows the trajectory of the soliton moving from $z = 0$ to the turning point $z = L$ in the interval $t = T/4$, where T is the period of a complete oscillation. The turning point, which determines the amplitude of the soliton oscillation, can be explicitly calculated by the position where the velocity vanishes $V(z = L) = 0$. Using the relation $\epsilon(L) = \epsilon_0$, we have $L/R_z = \sqrt{1 - (1 - U_0^2)^{1/3}}$ which is plotted in Fig. 3(a) as a function of the initial velocity. Direct integration of Eq. (11) from $z = 0$ to $z = L$ gives the result

$$\frac{T}{T_z} = \frac{4}{\pi} \sqrt{\frac{g}{\delta g}} \int_0^{L/R_z} \frac{v(\beta)d\beta}{\sqrt{v^3(\beta) - 1 + U_0^2}}, \quad (12)$$

for the period of the soliton oscillation, with $v(\beta) = 1 - \beta^2$ and $\beta = z/R_z$. The integral in Eq. (12) can be solved analytically in two extreme cases: (i) The slowly moving soliton. For $U_0 \rightarrow 0$, the above integral can be solved with the help of Taylor expansions. Calculation gives the turning position as $L/R_z = U_0/\sqrt{3}$ and the oscillation period reads $T/T_z = 2\sqrt{g/3\delta g}$, showing that, in contrast to the usual dark solitons, the oscillation period of the magnetic soliton depends on the interaction parameters.

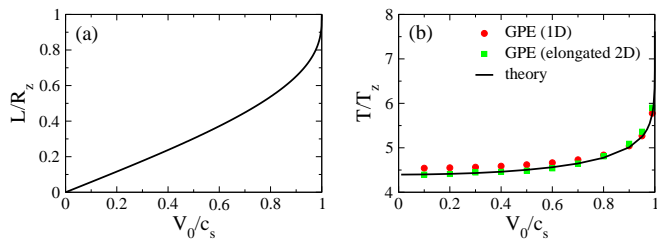


FIG. 3: In-trap oscillation of a magnetic soliton. (a) The turning position L/R_z is plotted as a function of the initial velocity V_0/c_s of the magnetic soliton created at the center of the harmonic trap. (b) The black line is the theoretical prediction of the scaled oscillation period T/T_z . The red circles and green squares are the data from the numerical solution of GPE for a trapped gas of ^{23}Na atoms in a 1D or an elongated 2D geometry with chemical potential $\mu = h \times 1210\text{Hz}$ and longitudinal trapping frequency $\omega_z = 2\pi \times 13\text{Hz}$. The transverse frequency for the 2D system is $\omega_y = 2\pi \times 130\text{Hz}$, thus $\mu = 9.3\omega_y$. The s -wave scattering lengths are $a_{11} = a_{22} = 54.54a_0$, $a_{12} = 50.78a_0$ with a_0 the Bohr radius.

(ii) The other interesting limiting case is for $U_0 \rightarrow 1$, that is when the velocity of the magnetic soliton approaches the spin sound velocity. In this case $L/R_z \rightarrow 1$ and we find $T/T_z = 2\sqrt{g/\delta g}$, which is $\sqrt{3}$ times larger than that in the slow moving limit. We emphasize that in this extreme case, the magnetic soliton will reach the edge of the Bose gas where the above approximation is no longer applicable [18].

For other intermediate values of initial velocities, the oscillation period is obtained by a direct numerical integration of Eq. (12) and the result is shown in Fig. 3(b). Here we have used the typical values of the scattering lengths of ^{23}Na where $\delta g/g \approx 0.07$. The oscillation period for small velocity is about 4.4 times of T_z which is much larger than the period $T/T_z = \sqrt{2}$ of a dark soliton in a single component Bose gas [17, 18]. The above prediction for the oscillation period of the magnetic soliton very well agrees with the numerical simulation of the GPE for a 1D condensate, as well as for a highly elongated 2D configuration.

Stability in two dimensions.—For a 2D system, when the transverse size of the condensate is larger than the width of the magnetic solitons, the solitons become unstable and start to bend while moving due to the snake instability. Since the width of magnetic solitons increases with their velocity, fast moving solitons are more stable than slow moving solitons. To showcase the instability of the magnetic solitons at low velocities, we plot the 2D density distributions of the first component n_1 in a harmonic trap obtained from the numerical simulation of the GPE. The soliton is imprinted at the trap center at $t = 0$ with an initial velocity $V = 0.1c_s$ and imaged after a short evolution time $t = 29\text{ms}$. As shown in Fig. 4, with the increase of the chemical potential the transverse size of the condensate increases. For $\mu = 9.3\omega_y$, where ω_y is

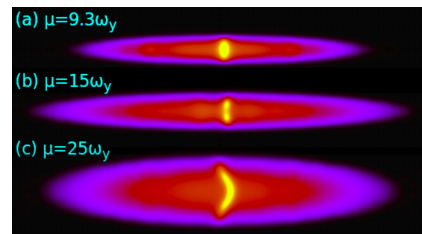


FIG. 4: Stability of magnetic solitons in 2D. The density distributions n_1 are shown for the following chemical potentials and aspect ratios $\lambda = R_z/R_y$: (a) $\mu = 9.3\omega_y$, $\lambda = 10$; (b) $\mu = 15\omega_y$, $\lambda = 10$; (c) $\mu = 25\omega_y$, $\lambda = 5$. In each case, the soliton is imprinted at the center of the Bose gas with an initial velocity of $V_0 = 0.1c_s$ along the horizontal z direction. The other parameters are the same as in Fig. 3.

the transverse trapping frequency, the magnetic soliton is stable and oscillates in trap in good agreement with the 1D result. For $\mu = 15\omega_y$, the magnetic soliton still moves and oscillates in the trap. However, vortex pairs soon appear in the second component and the system alternatively oscillates between a vortex pair and a magnetic soliton. For a 3D elongated harmonic trap, vortex rings are expected to appear and one consequently expects to observe an oscillating evolution between vortex ring and magnetic soliton configurations, in analogy with the oscillation between a vortex ring and a dark soliton already observed in a one-component Bose gas [19]. For $\mu = 25\omega_y$, the magnetic soliton is unstable, quickly starts to bend and eventually decays into vortices.

Conclusion.—We have investigated a magnetic soliton moving in a spinor Bose gas. The properties of the magnetic solitons and their oscillation dynamics in a harmonic trap are characterized and predicted analytically and numerically. We believe that our theoretical predictions will stimulate new experimental work in the field of spinor condensates. Since the relative phase of each magnetic soliton is π , a pair of solitons with opposite magnetization and moving in opposite directions could be engineered by imprinting a 2π relative phase between the two components, generating a domain wall of tunable width [14]. Other important questions, such as the stability analysis of magnetic solitons in higher dimensions, remain to be investigated in the future.

We thank G. Ferrari, G. Lamporesi, F. Dalfovo, A. Recati and M. Tylutki for stimulating discussions. This work was supported by ERC through the QGBE grant, by the QUIC grant of the Horizon2020 FET program and by Provincia Autonoma di Trento.

-
- [1] L. F. Mollenauer, R. H. Stolen, and J. P. Gordon, Phys. Rev. Lett. **45**, 1095 (1980).
 [2] W. P. Su, J. R. Schrieffer, and A. J. Heeger, Phys. Rev.

- Lett. **42**, 1698 (1979).
- [3] A. M. Kosevich, B. A. Ivanov, and A. S. Kovalev, Physics Reports **194**, 117 (1990).
- [4] S. Burger, K. Bongs, S. Dettmer, W. Ertmer, K. Sengstock, A. Sanpera, G. V. Shlyapnikov, and M. Lewenstein, Phys. Rev. Lett. **83**, 5198 (1999).
- [5] J. Denschlag *et al.*, Science **287**, 97 (2000).
- [6] L. Khaykovich, F. Schreck, G. Ferrari, T. Bourdel, J. Cubizolles, L. D. Carr, Y. Castin, C. Salomon, Science **296**, 1290 (2002).
- [7] Th. Busch and J. R. Anglin, Phys. Rev. Lett. **87**, 010401 (2001).
- [8] C. Becker, S. Stellmer, P. Soltan-Panahi, S. Dörscher, M. Baumert, E.M. Richter, J. Kronjäger, K. Bongs, and K. Sengstock, Nature Physics **4**, 496 (2008).
- [9] C. Hamner, J. J. Chang, P. Engels, and M. A. Hoefer, Phys. Rev. Lett. **106**, 065302 (2011).
- [10] A. M. Kamchatnov and V. V. Sokolov, Phys. Rev. A **91**, 043621 (2015).
- [11] S. Knoop, T. Schuster, R. Scelle, A. Trautmann, J. Appmeier, M. K. Oberthaler, E. Tiesinga, and E. Tiemann, Phys. Rev. A **83**, 042704 (2011).
- [12] In the case of ^{41}K and ^{87}Rb , one should instead consider the states $|F = 1; m_F = -1\rangle$ and $|F = 1; m_F = 0\rangle$ in order to ensure the positiveness of δg . In this case $g_{11} \approx g_{22}$ and $\delta g/g \approx 0.013$ and 0.0025 for the two atomic species, respectively.
- [13] A. M. Kamchatnov, Y. V. Kartashov, P.-É. Larré, and N. Pavloff, Phys. Rev. A **89**, 033618 (2014).
- [14] D. T. Son and M. A. Stephanov, Phys. Rev. A **65**, 063621 (2002).
- [15] Note that in this 1D description, $n_{1,2}$ are the numbers of atoms per unit length and g_{jl} are the 1D coupling constants. In a cylindrical harmonic trap, they are expressed in terms of the scattering lengths as $g_{jl} = 2a_{jl}\hbar\omega_{\perp}$. See [16], Ch.24.
- [16] L. P. Pitaevskii and S. Stringari, *Bose-Einstein Condensation and Superfluidity*, (Oxford University Press, New York, 2016).
- [17] Th. Busch and J. R. Anglin, Phys. Rev. Lett. **84**, 2298 (2000).
- [18] V. V. Konotop and L. Pitaevskii, Phys. Rev. Lett. **93**, 240403 (2004).
- [19] I. Shomroni, E. Lahoud, S. Levy and J. Steinhauer, Nature Physics **5**, 193 (2009).